



A VISCOELASTIC DYNAMIC VIBRATION ABSORBER WITH ADAPTABLE SUPPRESSION BAND: A FEASIBILITY STUDY

Y. KETEMA

*Department of Aerospace Engineering and Mechanics, University of Minnesota,
Minneapolis, MN 55455, U.S.A.*

(Received 1 December 1997, and in final form 16 April 1998)

A semi-active dynamic vibration absorber with an array of viscoelastic elements is studied. The viscoelastic elements are modelled as materials with memory in which the internal dissipative forces depend on current, as well as previous deformations. The viscoelastic behavior is governed by two parameters: the relaxation modulus G_0 , and the relaxation time γ . The principle of time-temperature superposition is used to affect a dependence of the relaxation time γ on temperature. It is shown that this temperature dependence can be utilized to design a dynamic vibration absorber whose suppression band can be shifted towards larger or smaller frequencies, thereby creating an effective suppression band considerably wider than that of a conventional dynamic vibration absorber.

© 1998 Academic Press

1. INTRODUCTION

Dynamic vibration absorbers are important means of providing vibration suppression in many mechanical systems especially near resonance. Examples of such systems include machines, heavy duty vehicles, generators, and building structures. For a detailed account of such applications and further references, the reader is referred to reference [1].

An important attribute of a dynamic absorber is its suppression band—the frequency range where the transfer function between the driving force and the oscillations of the main system has magnitude smaller than unity. The problem of the suppression band was first considered by Roberson [2] who studied a dynamic vibration absorber with a linear and a cubic spring in parallel, and showed that such a non-linear dynamic vibration absorber had a wider suppression band than the linear vibration absorber. At about the same time, a non-linear dynamic vibration absorber with a hardening spring of hyperbolic sine characteristic was studied in reference [3], and again it was shown that this dynamic vibration absorber has a wider suppression band than the linear dynamic vibration absorber. However, partly due to the rather impractical nature of these set-ups, several studies have since then been devoted to obtaining alternative dynamic vibration absorbers with broad suppression bands.

A broadband non-linear dynamic vibration absorber with a softening spring of Belleville type is considered in reference [4]. It is shown that in this case a suppression band that is roughly 10% of the tuning frequency can be obtained. However, the suppression band is not located about the resonance frequency of the main system. In fact, at the resonance frequency, the amplitude of the main system is larger than it would be with an undamped linear vibration absorber.

In reference [5], another non-linear dynamic vibration absorber—an impact vibration absorber—is studied. This consists of a small rigid mass in a container that is firmly attached to the main mass. The mass may collide with the walls of its container during the motion of the system, which accounts for the non-linearity. This non-linear dynamic vibration absorber has the advantage of not exhibiting the amplitude peaks that are generated by a linear vibration absorber on both sides of the resonance frequency. However, it has a smaller suppression band than that of a linear dynamic vibration absorber.

A general point of concern with non-linear dynamic vibration absorbers is that they may lead to instabilities with unwanted consequences. This has been pointed out in reference [6] where non-linear dynamic vibration absorbers with both hardening and softening cubic characteristics are studied.

More recently, dynamic vibration absorbers with viscoelastic materials were studied in reference [7], and the temperature dependence of such absorbers was investigated. The suppression band of the viscoelastic dynamic vibration absorber is comparable to that of a conventional dynamic vibration absorber, and therefore leads to the same concerns that are associated with the latter.

The aim of the present paper is to make use of the temperature dependent mechanical behavior of viscoelastic materials to design a dynamic vibration absorber with an adaptable suppression band. The material-with-memory model is used to describe the viscoelastic behavior and its temperature dependence. The adaptability of the suppression band allows for the dynamic vibration absorber to keep providing vibration suppression as, for example, the driving frequency, or the natural frequency of the main system, fluctuates. It is shown that, in this way, a significantly wider suppression band can be obtained than from an optimized damped linear vibration absorber. This suppression band is generally centered at the resonance frequency which is an advantage over e.g., the non-linear vibration absorber in reference [4]. This is therefore a study that contributes to the feasibility and advantage of the viscoelastic dynamic vibration absorber.

2. CONSTITUTIVE ASSUMPTIONS AND DYNAMICAL EQUATIONS

Consider the assembly shown in Figure 1 that consists of an oscillator of mass M , attached to a spring and dashpot, and a dynamic vibration absorber consisting of a mass m attached to the main system through an array of viscoelastic bars. The stiffness of the spring is denoted by k , and the damping constant of the dashpot is b . The viscoelastic bars are all assumed to have the same referential length L_0 . Let $x_i = \chi_i(X, t)$ denote the position of a particle X of the viscoelastic bar i at time t , where both x_i and X are measured relative to the fixed vertical wall in Figure 1. If one lets l_0 denote the undistorted length of the spring, it follows that for all i , $x_i(t) \equiv \chi_i(l_0, t) - l_0$ measures the elongation of the spring, and $x_2(t) \equiv \chi_i((l_0 + L_0), t) - l_0 - L_0$ measures the elongation of the viscoelastic bars. The deformation gradient history in bar i is given by

$$F_i(X, t - s) \equiv \frac{\partial \chi_i(X, t - s)}{\partial X}, \quad \forall s > 0.$$

The relative strain history for bar i is then characterized by

$$[J_i]_i(X, t - s) = \frac{[F_i(X, t - s)]^2}{[F_i(X, t)]^2} - 1, \quad \forall s \geq 0. \quad (1)$$

Assuming that the constitutive response function for determining the present value of the axial force $f_i(X, t)$ on the particle X in the viscoelastic bar i is of the finite-linear form, (see reference [8]), one has

$$f_i(X, t) = \bar{f}^e(F_i(X, t)) + \int_0^\infty \frac{dG_i(s)}{ds} [J_i]_i(X, t - s) ds, \quad (2)$$

where $\bar{f}^e(\cdot)$ denotes an elastic response function, here assumed to be the same for all the viscoelastic bars, and $G_i(\cdot)$ is the viscoelastic relaxation function for bar i .

The Piola–Kirchoff stress in bar i is given by $f_i(X, t)/A_0$, where A_0 is the referential cross-sectional area of the bar (assumed constant), and the balance of linear momentum requires

$$\frac{1}{A_0} \frac{\partial f_i(X, t)}{\partial X} = \rho_0 \ddot{\chi}_i(X, t), \quad (3)$$

where ρ_0 is the constant reference mass density, assumed to be the same for all bars. In this work, the inertia of the viscoelastic bars will be neglected. Then, $f_i(X, t)$ is independent of X from equation (3) and, as an approximation, the deformation of the bars may be assumed to be homogeneous, so that one may write

$$x_i = \chi_i(X, t) = l_0 + x_1(t) + (X - l_0)\xi_i(t), \quad (4)$$

where $\xi_i(t_0) = 1$ if bar i is unstretched at $t = t_0$. Clearly,

$$l_0 + L_0 + x_2(t) = \chi(l_0 + L_0, t) = l_0 + x_1(t) + L_0\xi_i(t), \quad (5)$$

and it follows that

$$\xi_i(t) = 1 + \frac{x_2(t) - x_1(t)}{L_0} \equiv \zeta(t) \quad (6)$$

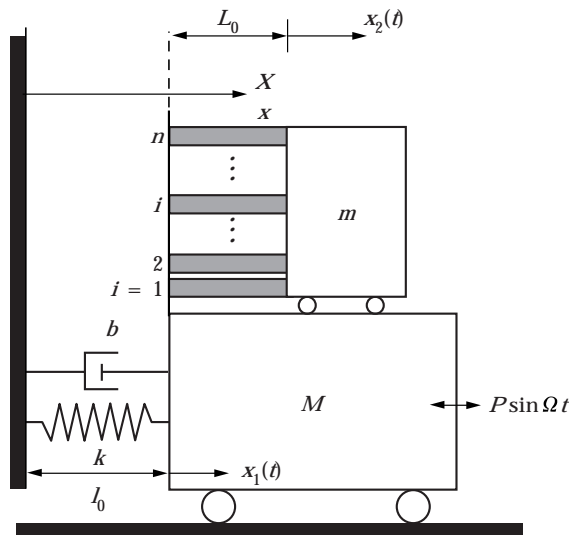


Figure 1. A dynamic vibration absorber with an array of viscoelastic bars.

is the same for all bars. Then, for all i , the deformation gradient $F_i(X, t) = \partial\chi_i(X, t)/\partial X = \xi(t)$ is the homogeneous stretch of material filaments so that

$$\bar{F}^e(F_i(X, t)) = f^e(\xi(t)), \quad (7)$$

and

$$[J_i](X, t - s) = \frac{\xi^2(t - s) - \xi^2(t)}{\xi^2(t)}. \quad (8)$$

Now, from equations (2), (7) and (8) it follows that $f_i(X, t) = f_i(t)$, where

$$f_i(t) = f^e(\xi(t)) + \int_0^\infty \frac{dG_i(s)}{ds} \frac{\xi^2(t - s) - \xi^2(t)}{\xi^2(t)} ds. \quad (9)$$

The dynamical equations for the masses M and m then take the form

$$M\ddot{x}_1(t) = -kx_1(t) - \mu\dot{x}_1(t) + \sum_{i=1}^n f_i(t) + P \sin \Omega t, \quad (10)$$

$$m\ddot{x}_2 = -\sum_{i=1}^n f_i(t). \quad (11)$$

3. TIME-TEMPERATURE SUPERPOSITION: REDUCED DYNAMICAL EQUATIONS

Suppose that the relaxation function for a viscoelastic bar corresponding to a reference temperature T_s is given by

$$G(s) = G_0 e^{-s/\gamma_0}, \quad (12)$$

for $s \geq 0$, where $G_0 > 0$ is the relaxation modulus, and $\gamma_0 > 0$ is the relaxation time at this temperature[†]. Thus, both G_0 and γ_0 are assumed to be the same for all the viscoelastic bars. Then, according to a common application of the time-temperature superposition principle, (see reference [9]), the relaxation function $G(s, T)$ at temperature T is given by

$$G(s, T) = G\left(s \frac{\gamma_0}{\gamma(T)}\right) = G_0 e^{-s/\gamma(T)}, \quad (13)$$

where $\gamma(T_s) = \gamma_0$ and $\gamma(T) > 0$ decreases rapidly with increasing temperature, especially for a polymer near its glass transition temperature. This hypothesis reflects the experimental fact that the relaxation modulus itself does not notably depend on temperature, and that the temperature dependence of the relaxation function is adequately characterized by a temperature dependent relaxation time $\gamma(T)$.

For polymers, a widely used expression for $\gamma(T)$ is given by the Williams-Landel-Ferry formula (see e.g., references [10, 11]),

$$\gamma(T) = \gamma_0 e^{\psi(T)}, \quad \psi(T) = \frac{c_1(T - T_s)}{c_2 + T - T_s}, \quad (14)$$

[†]This is a simplifying assumption for the behavior of the viscoelastic material. A more general model would be that involving a spectrum of relaxation times.

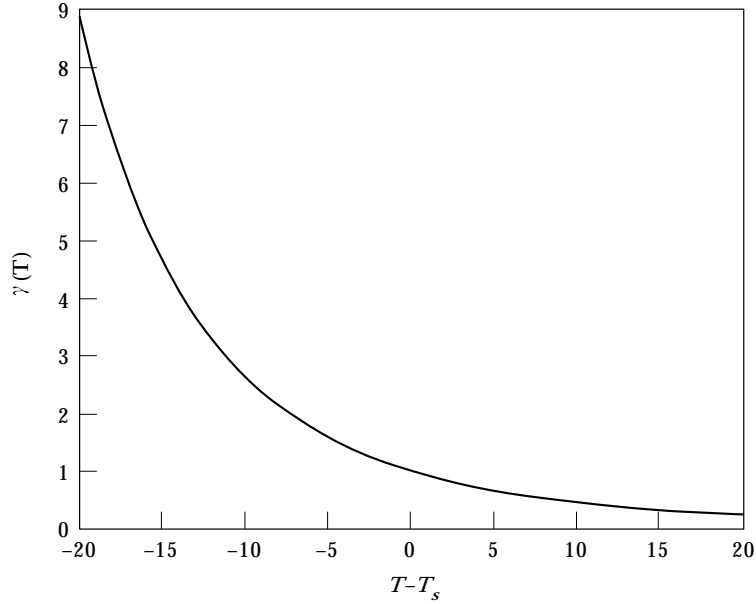


Figure 2. The normalized relaxation function for rubber: $\gamma(T)/\gamma_0 = e^{\psi(T)}$ versus temperature, $(T - T_s)$.

where the material constants c_1 and c_2 are positive and dependent on the reference temperature T_s . For rubbers, for example, this expression is fairly well approximated by the form

$$\psi(T) = \frac{-8.86(T - T_s)}{101.6 + T - T_s}, \quad (15)$$

where T_s is a material dependent reference temperature that normally lies about 50°K above the glass transition temperature, and thus lies roughly in the range of 200°K – 300°K . The large effect of temperature on the temperature dependent relaxation time $\gamma(T)$ of equation (14), (where $\psi(T)$ is given by equation (15)), is shown in Figure 2. Clearly, in order to double that value of $\gamma(T)$ with respect to its value γ_0 at $T = T_s$ a decrease of approximately 7°K is all that is necessary; to cut by one-half the value of $\gamma(T)$ would take only an increase of 10°K .

Denoting the temperature in bar i by T_i the relaxation function in bar i is

$$G_i(s) = G(s, T_i) = G_0 e^{-s/\gamma(T_i)}. \quad (16)$$

Then, using equation (16) in equation (9), it follows that the force throughout the viscoelastic bar i is

$$f_i(t) = f^e(\xi(t)) - \frac{G_0}{\gamma(T_i)} \int_0^\infty e^{-s/\gamma(T_i)} \frac{\xi^2(t-s) - \xi^2(t)}{\xi^2(t)} ds, \quad (17)$$

and by introducing the auxiliary function $\zeta_i(t)$ through

$$\zeta_i(t) = \int_0^\infty e^{-s/\gamma(T_i)} \frac{\xi^2(t-s) - \xi^2(t)}{\xi^2(t)} ds, \quad (18)$$

one may rewrite the dynamical equations (10) and (11) equivalently as the system

$$\begin{aligned} M\ddot{x}_1(t) &= -kx_1(t) - \mu\dot{x}_1(t) + P \sin \Omega t + n f^e(\zeta(t)) - \sum_{i=1}^n \frac{G_0}{\gamma(T_i)} \zeta_i(t), \\ m\ddot{x}_2(t) &= -n f^e(\zeta(t)) + \sum_{i=1}^n \frac{G_0}{\gamma(T_i)} \zeta_i(t), \end{aligned} \quad (19)$$

$$\dot{\zeta}_i(t) = - \left[\frac{1}{\gamma(T_i)} + \frac{2\dot{\zeta}(t)}{\zeta(t)} \right] \zeta_i(t) - \gamma(T_i) \frac{2\dot{\zeta}(t)}{\zeta(t)}.$$

Next, defining the referential elastic modulus

$$k_e \equiv \frac{df^e}{d\zeta}(1) > 0, \quad (20)$$

and linearizing the system (19) about the undistorted state, $x_1 = x_2 = 0$, $\zeta = 1$, one readily finds

$$\begin{aligned} M\ddot{x}_1(t) &= -kx_1(t) - b\dot{x}_1(t) + nk_e(x_2(t) - x_1(t)) - \sum_{i=1}^n \frac{G_0}{\gamma(T_i)} \zeta_i(t) + P \sin \Omega t, \\ m\ddot{x}_2(t) &= -nk_e(x_2(t) - x_1(t)) + \sum_{i=1}^n \frac{G_0}{\gamma(T_i)} \zeta_i(t), \\ \dot{\zeta}_i(t) &= -\frac{1}{\gamma(T_i)} \zeta_i(t) - 2 \frac{\gamma(T_i)}{L_0} (\dot{x}_2(t) - \dot{x}_1(t)). \end{aligned} \quad (21)$$

4. DYNAMIC CHARACTERISTICS OF THE ABSORBER

For what follows, it is convenient to non-dimensionalize the equations of motion. Thus, a dimensionless time τ is introduced through

$$t = \frac{\tau}{\omega_0}, \quad (22)$$

where $\omega_0 = \sqrt{k/M}$, i.e., the natural frequency of the undamped main oscillator. Also the following dimensionless parameters are defined:

$$\delta = \frac{b}{k}, \quad \kappa = \frac{k_e}{k}, \quad \Phi_0 = \frac{G_0}{kL_0}, \quad \alpha = \frac{M}{m}, \quad p = \frac{P}{kL_0}, \quad \omega = \frac{\Omega}{\omega_0}. \quad (23)$$

The position variables $x_1(t)$ and $x_2(t)$ are scaled by the undistorted length of the viscoelastic bar L_0 so that

$$\tilde{x}_1(\tau) = \frac{x_1(\tau/\omega_0)}{L_0}, \quad \tilde{x}_2(\tau) = \frac{x_2(\tau/\omega_0)}{L_0}. \quad (24)$$

For each $\zeta_i(t)$, a non-dimensional variable is defined through

$$\tilde{\zeta}_i = \frac{\zeta_i}{\gamma(T_i)}. \quad (25)$$

Next, using equation (23), (24) and (25) in equation (21) gives the dimensionless equations

$$\begin{aligned} \ddot{\tilde{x}}_1(\tau) &= -\tilde{x}_1(\tau) + \delta\dot{\tilde{x}}_1(\tau) + n\kappa(\tilde{x}_2(\tau) - \tilde{x}_1(\tau)) - \Phi_0 \sum_{i=1}^n \tilde{\zeta}_i(\tau) + p \sin \omega\tau, \\ \ddot{\tilde{x}}_2(\tau) &= -n\alpha\kappa(\tilde{x}_2(\tau) - \tilde{x}_1(\tau)) + \alpha\Phi_0 \sum_{i=1}^n \tilde{\zeta}_i(\tau), \\ \dot{\tilde{\zeta}}_i(\tau) &= -\frac{1}{\gamma(T_i)\omega_0} \tilde{\zeta}_i(\tau) - 2(\dot{\tilde{x}}_2(\tau) - \dot{\tilde{x}}_1(\tau)), \end{aligned} \quad (26)$$

where superposed dots now denote differentiation with respect to τ . In what follows, $\gamma(T_i)$ will be denoted by γ_i with the understanding that the value of γ_i may be changed through a change in the temperature T_i in accordance with the discussion in the previous section.

It is straightforward to show, for example by the method of Laplace transforms, that the solution to equation (26) takes the form

$$\tilde{x}_1(\tau) = X_1(\omega)p \sin \omega\tau, \quad \tilde{x}_2(\tau) = X_2(\omega)p \sin \omega\tau, \quad \tilde{\zeta}_i(\tau) = Z_i(\omega)p \sin \omega\tau, \quad (27)$$

where $X_1(\omega)$, $X_2(\omega)$, and $Z_i(\omega)$, are the sinusoidal transfer functions between the forcing $p \sin \omega\tau$ and $\tilde{x}_1(\tau)$, $\tilde{x}_2(\tau)$, and $\tilde{\zeta}_i(\tau)$ respectively, which are given by

$$X_1(\omega) = \frac{F_2(\omega)}{(-\omega^2 + \delta i\omega + 1)F_2(\omega) - \omega^2 F_1(\omega)}, \quad (28)$$

$$X_2(\omega) = \frac{\alpha F_1(\omega)}{\alpha F_1(\omega) - \omega^2}, \quad (29)$$

$$Z_i(\omega) = \frac{1}{1 + i\gamma_i\omega_0\omega} 2i\gamma_i\omega_0\omega(X_1(\omega) - X_2(\omega)), \quad (30)$$

where

$$F_1(\omega) = n\kappa + 2\Phi_0\sigma(\omega), \quad F_2(\omega) = \alpha F_1(\omega) - \omega^2, \quad \sigma(\omega) = \sum_{i=1}^n \frac{i\omega\gamma_i\omega_0}{1 + i\omega\gamma_i\omega_0}. \quad (31-33)$$

4.1. ADAPTABLE VIBRATION SUPPRESSION

The aim in designing a dynamic vibration absorber that provides optimal vibration suppression for some forcing frequency ω is to minimize $|X_1(\omega)|$. According to equation (28), this is equivalent to obtaining $F_2(\omega) = 0$. But it follows from equation (32) that one has $F_2(\omega) = 0$ only if $F_1(\omega)$ is real, and this requires $\sigma(\omega)$ to be real according to equation (31). On the other hand, $\sigma(\omega)$ is real if $\gamma_i\omega_0 \rightarrow \infty$ or $\gamma_i\omega_0 \rightarrow 0$ for each i , i.e., if each term in the sum defining $\sigma(\omega)$ in equation (33) is real.

Recall that the value of γ_i in bar i is dependent on the temperature in bar i . Indeed, according to equation (14), $\gamma_i\omega_0 \rightarrow \infty$ and $\gamma_i\omega_0 \rightarrow 0$ are obtained for large temperatures, and small temperatures respectively, in bar i . Due to the nature of the function $\gamma(T)$, these conditions can only be satisfied approximately. Nevertheless, they serve as guidelines for tuning the dynamic vibration absorber, and do lead to adequate results. This is shown in the next section, where the temperature changes necessary are also considered.

Suppose now that a number v of the viscoelastic bars, ($0 \leq v \leq n$), are at “low” temperatures such that for $1 \leq i \leq v$, $\gamma_i \omega_0 \gg 1$. In addition, let the rest $n - v$ bars be at “high” temperatures such that $\gamma_i \omega_0 \ll 1$ for $v + 1 \leq i \leq n$. It is then easy to show that

$$\sigma(\omega) = v + \mathcal{O}(\varepsilon), \quad (34)$$

where

$$\varepsilon = \max \left(\max_{1 \leq i \leq v} \left(\frac{1}{\gamma_i \omega_0 \omega} \right), \max_{v+1 \leq i \leq n} (\gamma_i \omega_0 \omega) \right). \quad (35)$$

Then,

$$F_2(\omega) \approx -\omega^2 + n\alpha\kappa + 2v\Phi_0\alpha, \quad (36)$$

which vanishes at

$$\omega^* = \sqrt{n\alpha\kappa + 2v\Phi_0\alpha}. \quad (37)$$

The dependence of ω^* on the number of viscoelastic bars at the lower temperature, v , allows one to control the frequency at which $F_2(\omega)$ approaches zero, and therefore the operating frequency of the dynamic vibration absorber. Clearly, the suppression band, which is a the neighborhood of the operating frequency, will also be shifted with a change of v . Hence, one has a dynamic vibration absorber with adaptable suppression band.

4.2. EXAMPLES

Suppose a dynamic vibration absorber has two viscoelastic elements and that it is to operate in a frequency interval around $\omega = 1$, i.e., the resonance frequency of the main system. Let, for example, $\Phi_0 = 0.005$, $\alpha = 10$ and $\kappa = 0.045$. Then, from equation (37), one sees that $\omega^* = 1$, (i.e., maximum vibration suppression is obtained at $\omega = 1$), if one

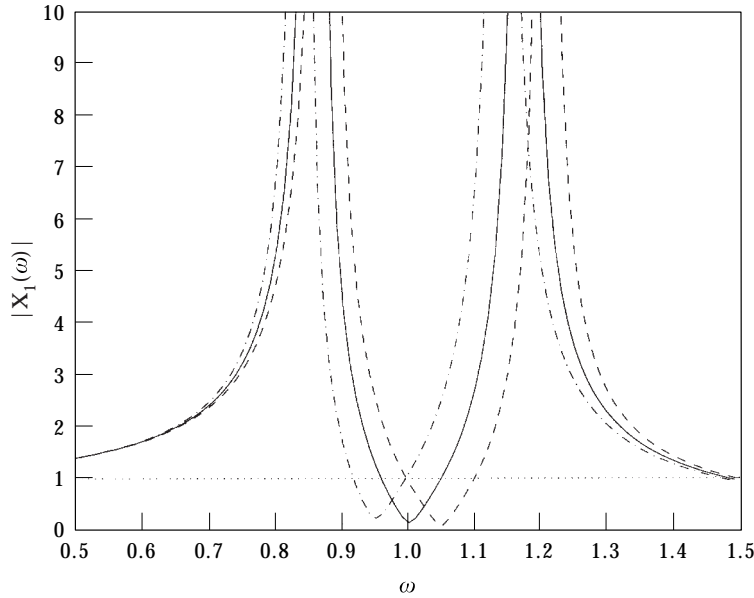


Figure 3. Amplitude versus frequency for the main mass with $n = 2$, $\Phi_0 = 0.005$, $\kappa = 0.045$, $\alpha = 10$ and $v = 0$ (— · —), $v = 1$ (—), $v = 2$ (— · — · —).

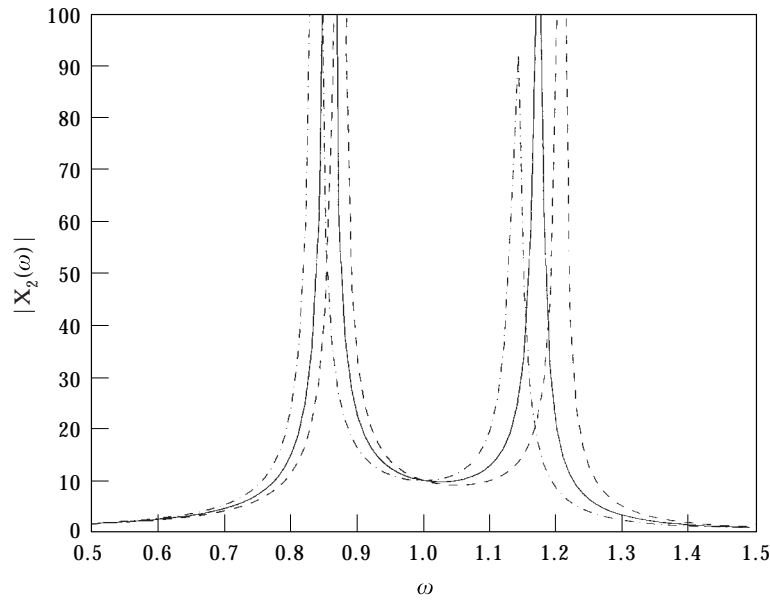


Figure 4. Amplitude versus frequency for the absorber mass with $n = 2$, $\Phi_0 = 0.005$, $\kappa = 0.09$, $\alpha = 10$ and $v = 0$ (— · —), $v = 1$ (—), $v = 2$ (---).

chooses $v = 1$. Also, for $v = 0$, one has $\omega^* = 0.949$ and $\omega^* = 1.049$ for $v = 2$. This result is illustrated in Figure 3, where the magnitude of the transfer function for the main mass, $|X_1(\omega)|$, is plotted against the forcing frequency for the cases $v = 0$, $v = 1$ and $v = 2$. Note that by changing v between 0, 1 and 2, it is possible to keep $|X_1(\omega)| < 1$ for ω between approximately 0.92 and 1.1, thereby creating a suppression band approximately twice as wide as for the case of, for example, $v = 1$. The corresponding magnitude of the transfer

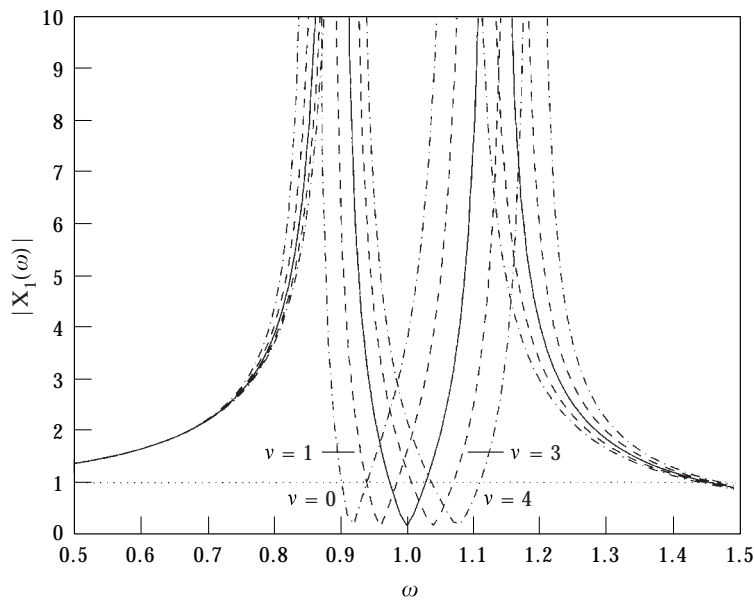


Figure 5. Amplitude versus frequency for the main mass with $n = 4$, $\Phi_0 = 0.004$, $\kappa = 0.021$ and $\alpha = 10$ for $v = 0, 1, 2, 3, 4$; $v = 2$ (—).

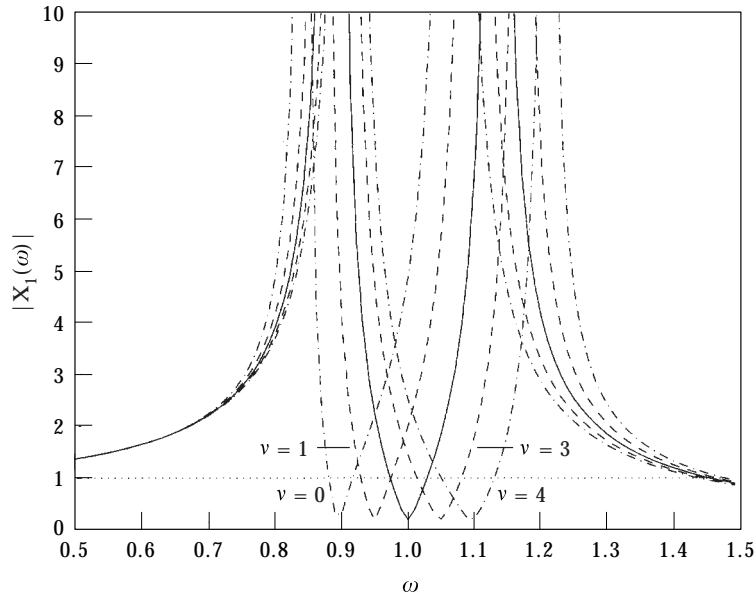


Figure 6. Amplitude versus frequency for the main mass with $n = 4$, $\Phi_0 = 0.005$, $\kappa = 0.02$ and $\alpha = 10$ for $\nu = 0, 1, 2, 3, 4$; $\nu = 2$ (—).

function for the absorber mass is shown in Figure 4. The larger and smaller values of $\gamma_i\omega_0$, (corresponding to $\gamma_i\omega_0 \rightarrow \infty$ and $\gamma_i\omega_0 \rightarrow 0$ respectively), that are used in these calculations are 20 and 0.1, respectively.

A slightly larger effective suppression band can be obtained with four viscoelastic bars, i.e., $n = 4$. Let $\Phi_0 = 0.004$, $\alpha = 10$, and $\kappa = 0.021$. Then, from equation (37), it follows that $\omega^* = 1$ for $\nu = 2$. Also, for $\nu = 0$ and $\nu = 1$, $\omega^* < 1$ while $\omega^* > 1$ for $\nu = 3$ and $\nu = 4$. The corresponding amplitude versus frequency diagrams are shown in Figure 5. The larger and smaller values of $\gamma_i\omega_0$, that are used in this example are 20 and 0.01, respectively.

A third example is shown in Figure 6 with $n = 4$ but with $\Phi_0 = 0.005$, $\alpha = 10$, and $\kappa = 0.02$. Also in this case $\omega^* = 1$ for $\nu = 2$. For $\nu = 0$ and $\nu = 1$, $\omega^* < 1$ while $\omega^* > 1$ for $\nu = 3$ and $\nu = 4$. Note that a larger suppression band than in Figure 5 is obtained to the right of $\omega = 1$. At the same time, however, a "hole" has been created in the suppression band to the left of $\omega = 1$. Also in this example, the larger and smaller values of $\gamma_i\omega_0$ used are 20 and 0.01, respectively.

In conclusion, an increase in Φ_0 leads in general to a larger effective suppression band because a larger change of ω^* is obtained with a unit change in ν according to equation (37). On the other hand an increase in n shrinks the suppression band of the absorber for each ν , which is clear from a comparison of equations (3) and (5). Nevertheless a larger n may be beneficial to the effective suppression band, as shown in Figure 6.

The effective suppression bands of the dynamic vibration absorber obtained in the cases above are all roughly 10% or higher of the tuning frequency assumed to be at 1. This can be compared, for example, to the suppression band of the optimized damped linear dynamic vibration absorber given in reference [12]. There, an optimal suppression band that is roughly 5% of the tuning frequency, (approximately 0.98), was obtained with the same mass ratio $\alpha = 10$.

To understand the role of the mass ratio α , and because in many practical applications a larger value of α may be required, a fourth example is shown in Figure 7. Here, $\alpha = 40$,

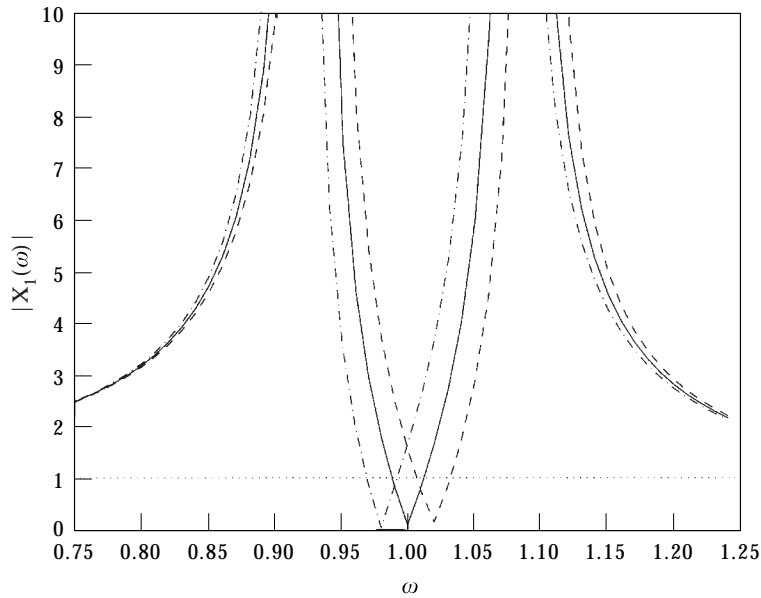


Figure 7. Amplitude versus frequency for the main mass with $n = 2$, $\Phi_0 = 0.005$, $\kappa = 0.012$, $\alpha = 40$ and $v = 0$ (---), $v = 1$ (—), $v = 2$ (---).

$\kappa = 0.012$, $\Phi_0 = 0.005$, and $n = 2$. The solid line corresponds to $v = 1$ while the dashed-dotted and dashed lines correspond to $v = 2$ and $v = 0$, respectively. A comparison of Figure 7 to Figure 3 shows that each amplitude curve in Figure 7 has a narrower suppression band than the corresponding curve in Figure 3. This is a direct result of the higher value of α . However, the qualitative behavior of the absorber has not changed; it is still possible to affect an adaptive suppression band by choosing the number of bars at the higher temperature, v , appropriately.

To get a rough estimate of the changes in temperature needed to realize the above effects, suppose that $\omega_0 = 10$ rad/s and that the viscoelastic bars are made of a material with $\gamma = 2s$

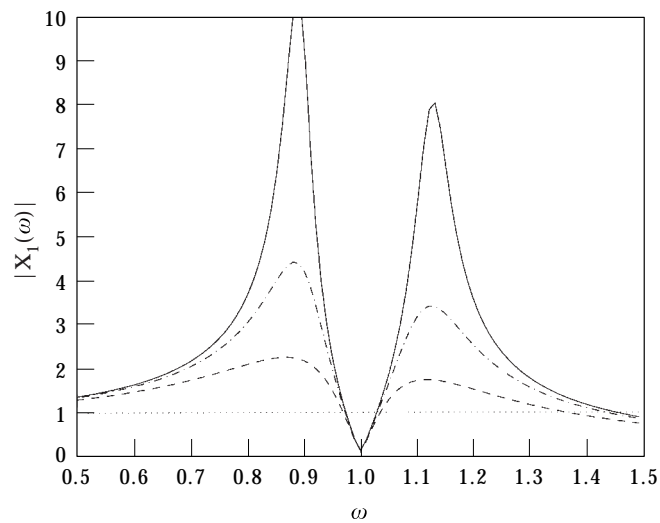


Figure 8. Amplitude versus frequency for the main oscillator with $n = 4$, $v = 2$, $\Phi_0 = 0.0035$, $\kappa = 0.0215$ and $\alpha = 10$; $\delta = 0$ (—), $\delta = 0.25$ (---), $\delta = 0.5$ (---).

at 296.8°K , with $T_s = 360^\circ\text{K}$. (This corresponds to $\gamma_0 = 1.89 \times 10^{-6}\text{s}$ according to equation (14)). Note that, for bar i , $\gamma_i\omega_0 = 20$ at 296.8°K . Now, using $\gamma_0 = 1.89 \times 10^{-6}\text{s}$ in equation (14), it follows that, in order to decrease $\gamma_i\omega_0$ to 0.1, an increase in the temperature T_i of 12°K is all that is necessary. On the other hand, to decrease $\gamma_i\omega_0$ to 0.01, it takes a 20°K -increase in T_i .

4.3. THE EFFECT OF VISCOUS DAMPING

The effect of viscous damping is to generally decrease the amplitude at all frequencies. At large damping coefficients (say $\delta > 0.5$) this results in a slight increase in the width of the suppression band. This is shown in Figure 8 where $|X_1(\omega)|$ is plotted against the forcing frequency for $n = 4$, $\nu = 2$, $\Phi_0 = 0.0035$, $\kappa = 0.0215$, $\alpha = 10$ and for of the dimensionless damping coefficient $\delta = 0$, $\delta = 0.25$ and $\delta = 0.5$.

5. CONCLUSION

Dynamic vibration absorbers are attractive devices for several reasons. The narrowness of the suppression band of conventional linear dynamic vibration absorbers, however, and the instabilities that may be introduced by non-linear dynamic vibration absorbers, are major concerns in their implementation.

The results in this paper suggest the possibility of using viscoelastic materials to design a semi-active dynamic vibration absorber with the stability of the linear dynamic vibration absorber but with a wider effective suppression band. The fact that the suppression band is easily centered at the resonance frequency is an additional advantage over non-linear dynamic vibration absorbers and conventional damped linear vibration absorbers.

Though the properties of rubber were used as an example of viscoelastic behavior in this paper, the practical implementation of the vibration absorber should be considered in the light of the wide variety of elastomers that can be manufactured with suitable prescribed qualities, both regarding mechanical and thermodynamic behavior. This greatly increases the feasibility of the viscoelastic dynamic vibration absorber.

A problem that requires further study is the effect of the non-linearity of the forces from the viscoelastic bars that may be important for large forcing amplitudes. In addition, only isothermal motions of the viscoelastic bars has been considered in this paper, i.e., heat generation inside the bars has been neglected. These points will be the subjects of future work.

REFERENCES

1. J. B. HUNT 1979 *Dynamic Vibration Absorbers*. London: Mechanical Engineering Publications Ltd.
2. R. E. ROBERSON 1952 *Journal of Franklin Institute* **254**, 205–220. Synthesis of a non-linear dynamic vibration absorber.
3. L. A. PIPES 1953 *Journal of Applied Mechanics* **20**, 515–518. Analysis of a non-linear dynamic vibration absorber.
4. J. B. HUNT and J. C. NISSEN 1982 *Journal of Sound and Vibration* **82**, 573–578. The broadband dynamic vibration absorber.
5. S. E. SEMERCIGIL, D. LAMMERS and Z. YING 1992 *Journal of Sound and Vibration* **156**, 445–459. A new tuned vibration absorber for wide band excitations.
6. S. NATSIAVAS 1992 *Journal of Sound and Vibration* **156**, 227–245. Steady state oscillations and stability of nonlinear dynamic vibration absorbers.
7. Y. SATOH 1993 *Nippon Kikai Gakkai Ronbunshu, C Hen.* **59**, 2968–2974. Influence of temperature dependence of the dynamic absorber elements on the vibration reduction characteristics.

8. B. D. COLEMAN and W. NOLL 1961 *Rev. Modern Phys.* **33**, 239–249. Foundations of linear viscoelasticity.
9. R. M. CHRISTENSEN 1982 *Theory of Viscoelasticity*. New York: Academic Press; second edition.
10. J. D. FERRY 1970 *Viscoelastic Properties of Polymers*. New York: John Wiley & Sons; second edition.
11. D. F. MOORE 1993 *Viscoelastic Machine Elements*. Oxford: Butterworth-Heinemann.
12. I. N. JORDANOV and B. I. CHESHANKOV 1988 *Journal of Sound and Vibration* **123**, 157–170. Optimal Design of linear and nonlinear dynamic vibration absorbers.

APPENDIX: NOMENCLATURE

$F_i(X, t - s)$	deformation gradient history in bar i
$[J_i]_i(X, t - s)$	relative strain history in bar i
L_0	undistorted lengths of viscoelastic bars
l_0	undistorted length of spring
M, m	primary and absorber masses
$\alpha = M/m$	mass ratio
k	stiffness of main system spring
$G(s)$	relaxation function for a viscoelastic bar
G_0	relaxation modulus for a viscoelastic bar
$\Phi_0 = G_0/(kL_0)$	non-dimensional relaxation modulus
T	temperature
γ	relaxation time for a viscoelastic bar
$\tilde{x}_{1,2}$	non-dimensional displacement from equilibria of main mass and absorber
ζ_i	non-dimensional auxiliary variable representing history of motion
n	number of viscoelastic bars
v	number of viscoelastic bars at the higher temperature
ω	non-dimensional forcing frequency
$\omega_0 = \sqrt{k/M}$	natural frequency of main system
$\kappa = k_e/k$	stiffness ratio of viscoelastic bar and main system spring
$p = P/(kL_0)$	non-dimensional forcing amplitude